

# Intestinal O<sub>2</sub> Consumption in Necrotizing Enterocolitis: Role of Nitric Oxide

PHILIP T. NOWICKI, KRISTINA M. REBER, PETER J. GIANNONE, CRAIG A. NANKERVIS, SUE HAMMOND, GAIL E. BESNER, AND DONNA A. CANIANO

Department of Pediatrics [P.T.N., K.M.R., P.J.G., C.A.N.], Department of Surgery [G.E.B., D.A.C.], Ohio State University, Columbus, Ohio 43205; Department of Laboratory Medicine [S.H.], Children's Hospital, Columbus, Ohio 43205

**ABSTRACT:** We tested the hypothesis that inducible isoform of nitric oxide synthase (iNOS)-derived nitric oxide (NO) inhibits oxygen consumption (V<sub>O<sub>2</sub></sub>) in human intestine resected for necrotizing enterocolitis (NEC). Each NEC resection specimen was divided into two sections based on histologic appearance: healthy or diseased. Intestine removed from infants for reasons other than NEC was used as control. The tissue injury score (0–6, with 6 indicating complete necrosis) was 0.4 ± 0.2 in control tissue, 1.2 ± 0.4 in NEC-healthy tissue, and 4.6 ± 0.5 in NEC-diseased tissue. Prominent iNOS staining was present in villus enterocytes in NEC-healthy tissue but not in the other tissue types. Intestinal V<sub>O<sub>2</sub></sub> (per direct oximetry, in nM O<sub>2</sub>/min/g) was significantly greater in control tissue than in NEC-healthy or NEC-diseased tissues. Accumulation of NO into buffer bathing intestinal slices (in nM NO/μL/g) was greater in NEC-healthy tissue than control or NEC-diseased tissues. The specific iNOS antagonist L-N<sup>ω</sup>-(1-iminoethyl)-lysine (L-NIL) reduced buffer NO concentration 76% and increased V<sub>O<sub>2</sub></sub> by 90% in NEC-healthy tissue; however, L-NIL had no effect on NO or V<sub>O<sub>2</sub></sub> in control or NEC-diseased tissue. Addition of exogenous NO via S-nitroso-N-acetylpenicillamine depressed V<sub>O<sub>2</sub></sub> in NEC-healthy and control tissues but not NEC-diseased tissue. A significant correlation was present between buffer NO concentration and V<sub>O<sub>2</sub></sub> in NEC-healthy tissue. We conclude that iNOS-derived NO suppresses V<sub>O<sub>2</sub></sub> in intestine resected for NEC that demonstrates a relatively normal histology on light microscopy. (*Pediatr Res* 59: 500–505, 2006)

The inducible isoform of nitric oxide synthase (iNOS) has been demonstrated in human intestine resected for NEC and hence implicated in disease pathogenesis (1,2). iNOS-derived nitric oxide (NO) has also been proposed as relevant in the etiology of intestinal damage following hypotension (3), lipopolysaccharide administration (4), ischemia-reperfusion (5), sustained use of hyperalimentation (6), and inflammatory bowel disease (7). Many mechanisms have been proposed to explain the intestinal damage generated by iNOS-derived NO. NO can react with superoxide anion to form peroxynitrite, a highly cytotoxic radical; indeed, nitrotyrosine, the footprint of peroxynitrite, has been identified in intestine resected for inflammatory bowel disease or NEC (1,7). iNOS also activates proinflammatory cytokines and hence generates an inflamma-

tory response, whereas iNOS-derived NO causes enterocyte apoptosis (7,8).

Yet another putative mechanism by which NO might affect tissue viability is *via* its direct effect on cellular respiration. NO reversibly inactivates cytochrome *c* within the mitochondrial electron transport chain (9) and depresses tissue V<sub>O<sub>2</sub></sub> in heart, kidney, and skeletal muscle tissues (10–12). Accordingly, we hypothesized that iNOS-derived NO suppresses V<sub>O<sub>2</sub></sub> in human preterm intestine resected for NEC. To test this hypothesis, intestinal V<sub>O<sub>2</sub></sub> and NO production were measured under *in vitro* conditions in human intestine resected for NEC, as well as in human intestine resected from infants for reasons other than NEC.

## MATERIALS AND METHODS

**Pharmacological reagents.** SP was used to stimulate the activity of eNOS (13). Tumor necrosis factor (TNF)-α was used to induce endogenous iNOS activity (14). L-NNA was used to inhibit eNOS activity (15). L-NIL was used to selectively inhibit iNOS activity (16). SNAP was used as an exogenous NO source (17). Drugs were purchased from Sigma Chemical Co. (St. Louis, MO) and dissolved in Krebs buffer. All Krebs buffer used in this study was of the following composition (in mM): NaCl 118, KCl 4.5, CaCl<sub>2</sub> 2.5, MgSO<sub>4</sub> 1.2, KH<sub>2</sub>PO<sub>4</sub> 1.2, NaHCO<sub>3</sub> 25, 0.026 EDTA. Buffer pH was 7.43 ± 0.05 when aerated with 21% O<sub>2</sub>, 5% CO<sub>2</sub>, bal N<sub>2</sub> at 37°C, whereas buffer O<sub>2</sub> concentration was 222 ± 3 nM O<sub>2</sub>/mL.

**In vivo measurement of V<sub>O<sub>2</sub></sub>.** The Fick method was used to determine *in vivo* intestinal V<sub>O<sub>2</sub></sub> using previously described methods (18). Briefly, blood flow (Q) and the arteriovenous O<sub>2</sub> content difference (a – v O<sub>2</sub>) in a vascularly isolated, innervated 5-cm segment of pig ileum were measured and then V<sub>O<sub>2</sub></sub> was calculated as Q × (a – v O<sub>2</sub>).

**In vitro measurement of V<sub>O<sub>2</sub></sub>.** Ileum was removed from anesthetized piglets, opened in the longitudinal plane, and pinned within a cutting device that generated thin (~0.3 mm) slices of intestinal wall (19 ± 3 mg). Slices were placed into warmed aerated Krebs buffer for 1 h before initiating *in vitro* studies. The method of Xie *et al.* (17) was adapted to measure V<sub>O<sub>2</sub></sub> under *in vitro* conditions. A biologic O<sub>2</sub> monitor was used (YSI 5300, YSI Inc., Yellow Springs, OH) that consisted of a 10-mL glass chamber situated within a water bath (37°C) and over a magnetic stirrer. To the chamber were added 3 mL of warmed, aerated Krebs buffer, a magnetic stir bar, and the ileal tissue. A Clark-type polarographic O<sub>2</sub> electrode was situated within the buffer, the chamber sealed, and the stirrer activated. The rate of fall in buffer O<sub>2</sub> concentration was determined over 5 min. The tissue was then removed, blotted dry, and weighed. Measurements were carried out in duplicate in separate tissue slices and the average V<sub>O<sub>2</sub></sub> was expressed as nM O<sub>2</sub>/min/g tissue.

**Abbreviations:** DNP, 2,4-dinitrophenol; eNOS, endothelial nitric oxide synthase; L-NIL, L-N<sup>ω</sup>-(1-iminoethyl)-lysine; L-NNA, L-NG-nitroarginine; NEC, necrotizing enterocolitis; SNAP, S-nitroso-N-acetylpenicillamine; SP, substance P; V<sub>O<sub>2</sub></sub>, oxygen consumption

Received September 20, 2005; accepted November 21, 2005.  
Correspondence: Philip T. Nowicki, M.D., Columbus Children's Research Institute, 700 Children's Dr., Columbus, OH 43205; e-mail: nowickip@pediatrics.ohio-state.edu  
This work was funded by National Institutes of Health Grant DK 065306 (P.T.N.)

DOI: 10.1203/01.pdr.0000203094.27615.5f

**NO measurement technique.** Krebs buffer (1 mL) was added to each well of a 6-well plate and immediately thereafter an initial 50- $\mu$ L buffer sample was taken for NO analysis. A tissue slice was added to each well and the plate incubated at 37°C; thereafter, a second buffer sample was taken, the tissue slices were removed, blotted, and weighed. The NO concentration of conditioned buffer samples was determined by means of a Sievers NO Analyzer (Sievers Instruments, Boulder, CO) as previously reported (19). Paired observations were made for each perturbation and the average taken, and final data expressed as nM NO/ $\mu$ L/g tissue.

**Animal studies.** Studies were carried out in piglet intestine to confirm the accuracy and reproducibility of the *in vitro* technique to measure intestinal V<sub>O<sub>2</sub></sub> and to determine the dose-response relationships for the pharmacological agents used in the work. The Institutional Animal Care and Use Committee of Columbus Children's Research Institute approved all animal work. Piglets were studied within 6 h of birth and were never fed. Anesthesia was achieved with telezol (7.5 mg/kg i.m.) and xylazine (5 mg/kg i.m.).

The first protocol compared *in vivo* and *in vitro* V<sub>O<sub>2</sub></sub> measurements on the same portion of ileum tissue to compare *in vivo* and *in vitro* methods to measure V<sub>O<sub>2</sub></sub>. Intestinal V<sub>O<sub>2</sub></sub> was first measured *in vivo* by means of the Fick method; thereafter, the ileal tissue was removed, cut into slices, and *in vitro* V<sub>O<sub>2</sub></sub> measurement carried out. The second protocol determined the optimal incubation time for NO studies. Ileum was incubated in Krebs buffer at 37°C for 0–180 min and the NO concentration determined thereafter in conditioned buffer. In the third protocol, SP (10<sup>-10</sup>–10<sup>-7</sup> M) was added to separate wells to determine dose-response for SP as a stimulant for eNOS. In a subsequent study, L-NNA (10<sup>-10</sup>–10<sup>-7</sup> M) or vehicle were added before SP (10<sup>-8</sup> M) to determine the dose-response for L-NNA as an eNOS antagonist. The fourth protocol determined the dose-response relationship of L-NIL as a specific antagonist for iNOS activity in newborn intestine. iNOS activity was induced in ileal tissue slices *in vitro* by exposure to TNF- $\alpha$  (10 ng/mL in Ham's F-12 medium, incubation at 37°C for 12 h) and confirmed by immunohistochemistry. Thereafter, L-NIL (10<sup>-6</sup>–10<sup>-3</sup> M), L-NNA (5  $\times$  10<sup>-8</sup> M) or vehicle (buffer) was added to separate wells and the plates incubated for an additional 2 h. NO concentration was compared between fresh and conditioned media.

**Human study population.** Work involving human infants was approved by the Institutional Review Board of Children's Hospital and parental consent was obtained before recovery of tissue. One group consisted of infants who underwent intestinal resection for NEC, while another (control) was comprised of infants who underwent small bowel resection for diagnoses other than NEC (congenital bowel atresia or stenosis). All human data presented herein were collected from small intestine.

**Tissue procurement.** Tissue processing commenced within 30 min of resection. Each NEC specimen was divided into healthy and diseased portions based on gross appearance; to this end, an inflammatory or hemorrhagic serosal or mucosal exudate, or bowel wall discoloration were considered evidence of disease.

**Tissue preparation.** Pieces of human tissue were often irregular in shape. This circumstance prompted us to pre-prepare each piece by squaring off corners so that a rectangular tissue segment of consistent dimensions from infant to infant were produced. Tissue segments were cut into full-thickness, ~0.3-mm slices (average weight: 20  $\pm$  2 mg). Two slices cut from each tissue segment, selected randomly, were submitted for histologic examination. The rest were placed into warmed aerated Krebs buffer for a 1-h equilibration before study.

**Histologic analysis.** Tissue was fixed in 10% neutral buffered formalin for 24 h, processed, and stained with hematoxylin and eosin (H&E) or with MAb to eNOS or iNOS (1:500; BD Biosciences, San Diego, CA). Tissue injury was quantified using a scoring system that used six descriptors: 1) villus destruction; 2) loss of crypt architecture; 3) vascular congestion, *i.e.* red blood cell distension of submucosal or villus microvessels; 4) coagulative necrosis; 5) submucosal edema; and 6) thinning of the intestinal wall. Scoring of both samples from each tissue block was carried out in a blinded fashion by two investigators and the average taken.

**Protocol.** V<sub>O<sub>2</sub></sub> was measured *in vitro* in pairs of tissue slices exposed to SP (10<sup>-8</sup> M), SNAP (10<sup>-4</sup> M), L-NNA (5  $\times$  10<sup>-8</sup> M), L-NIL (10<sup>-4</sup> M), or vehicle (Krebs buffer). To this end, tissue slices were placed into warmed, aerated Krebs buffer that contained a single agent for 2 h; thereafter, the tissue was transferred to the O<sub>2</sub> monitor chamber for V<sub>O<sub>2</sub></sub> measurement. NO release by tissue into bathing buffer was measured on tissue slices other than those used in the V<sub>O<sub>2</sub></sub> studies. Wells were filled with Krebs buffer containing one of the following: SP (10<sup>-8</sup> M), SNAP (10<sup>-4</sup> M), L-NNA (5  $\times$  10<sup>-8</sup> M), L-NIL (10<sup>-4</sup> M), or vehicle (Krebs buffer). Tissue was incubated at 37°C for 2 h before removal of conditioned buffer for NO measurement.

**Statistical analysis.** ANOVA was used to determine statistical significance of the data. In all cases, post hoc Tukey B tests were carried out determine sites of significance when the ANOVA F-statistic was significant ( $p < 0.05$ ).

Regression analysis was carried out to determine the interaction between buffer NO concentration and tissue V<sub>O<sub>2</sub></sub>, between gestational age and tissue V<sub>O<sub>2</sub></sub>, and between feeding parameters and tissue V<sub>O<sub>2</sub></sub>. All data are presented as mean  $\pm$  SD.

**RESULTS**

**Animal data.** V<sub>O<sub>2</sub></sub> data generated *in vivo* (Fick method) and *in vitro* (direct oximetry) on the same piece of ileum was similar: *in vivo* 398  $\pm$  45 nM O<sub>2</sub>/min/g; *in vitro* 427  $\pm$  41 nM O<sub>2</sub>/min/g ( $n = 5$ ). These data confirmed the validity of the *in vitro* method for measurement of intestinal V<sub>O<sub>2</sub></sub>. Accumulation of NO within the bathing buffer increased as a function of incubation time, with a linear increase noted between 90 and 150 min; NO data (in nM NO/ $\mu$ L/g) were 10  $\pm$  1, 13  $\pm$  2, 14  $\pm$  2, 18  $\pm$  2, 28  $\pm$  3, 40  $\pm$  3, and 45  $\pm$  4 at 0, 30, 60, 90, 120, 150, and 180 min of incubation, respectively. A 2-h incubation period was thus used for all subsequent NO studies. SP increased ileal release of NO into the bathing buffer; NO data (in nM NO/g) were 42  $\pm$  4; 44  $\pm$  3, 52  $\pm$  6, 72  $\pm$  6,\* and 74  $\pm$  5\* following application of vehicle (control) or SP, 10<sup>-10</sup>–10<sup>-7</sup>M in whole log increments for 2 h ( $n = 3$ ; \* $p < 0.05$  versus control). SP at 10<sup>-8</sup> M was thus used for all subsequent studies. Optimal attenuation of SP-induced NO production occurred at 5  $\times$  10<sup>-8</sup> M L-NNA (82  $\pm$  6% reduction of buffer NO concentration). Ileal exposure to TNF- $\alpha$  (10 ng for 12 h) induced iNOS, as evidenced by immunohistochemistry (data not shown), as well as by an increase in medium NO concentration at the end of the 12-h incubation (in nM NO/ $\mu$ L/g): control, 49  $\pm$  7; TNF- $\alpha$ , 103  $\pm$  37\* ( $n = 3$ , \* $p < 0.05$ ). Optimal attenuation of iNOS activity by L-NIL occurred at 10<sup>-4</sup> M (75  $\pm$  8% reduction in subsequent NO accumulation in medium over the ensuing 2 h); in contrast, L-NNA (5  $\times$  10<sup>-8</sup> M) had no effect on subsequent NO accumulation within the medium, indicating that the dose of L-NNA that effectively reduced the SP-induced increase in NO accumulation had no effect on iNOS activity. Finally, L-NIL (10<sup>-4</sup> M) had no effect on SP-induced NO accumulation, confirming its selectivity for iNOS.

**Human data.** Demographic features of the two patient groups were dissimilar (Table 1). None of the NEC cases were clustered and none represented focal perforations, factors that might reflect unique pathogenetic mechanisms (20,21).

The tissue injury score was significantly different among the three tissue groups: control, 0.4  $\pm$  0.2; NEC-healthy, 1.2  $\pm$  0.4\*; NEC-diseased, 4.6  $\pm$  0.5\*§ (\* $p < 0.01$ , NEC-healthy versus control; § $p < 0.01$  NEC-diseased versus NEC-healthy). eNOS was present in all control and NEC-healthy

**Table 1. Demographic characteristics of patient groups**

	Control infants ( $n = 7$ )	NEC infants ( $n = 14$ )
Gestational age (wk)	37 $\pm$ 5	27 $\pm$ 4*
Birth weight (g)	3590 $\pm$ 723	975 $\pm$ 287*
Age at laparotomy (d)	1 $\pm$ 2	17 $\pm$ 7*
Duration of feeding (d)	None fed	9 $\pm$ 4
Maximal feed volume (mL/kg/d)	None fed	48 $\pm$ 12

Data are given as mean  $\pm$  SD; \* $p < 0.01$  vs control group.

tissues and was exclusively localized to the microvasculature; in contrast, very little eNOS staining was present in NEC-diseased tissue (Fig. 1). iNOS was present in all NEC-healthy tissue specimens and was localized to villus enterocytes, and to a lesser extent the microvasculature; in contrast, iNOS was not present in any control tissue and was present to a limited extent in NEC-diseased tissue (Fig. 2).

Baseline  $V_{O_2}$  was significantly lower in the NEC-healthy or NEC-diseased tissues than in the control tissue (Table 2). L-NIL, L-NNA, or SP did not alter  $V_{O_2}$  in control tissue; in contrast, SNAP reduced  $V_{O_2}$  in control tissue by 44%. In NEC-healthy tissue, L-NIL increased  $V_{O_2}$  by 90%. Neither L-NNA nor SP altered  $V_{O_2}$  in the NEC-healthy tissue, whereas SNAP decreased  $V_{O_2}$  by 21% therein. None of the agents significantly altered  $V_{O_2}$  in the NEC-diseased tissue.

The concentration of NO in conditioned buffer at the end of the 2-h incubation period was significantly greater in the NEC-healthy tissue when compared with either control or NEC-diseased tissues (Table 3). L-NIL significantly reduced buffer NO concentration in the NEC-healthy tissue, whereas neither L-NNA nor SP had a significant effect. The buffer NO concentration in the control or NEC-diseased tissue groups was not affected by L-NIL, L-NNA, or SP. As expected, the addition of exogenous NO *via* SNAP increased buffer NO concentration in all groups.

A significant inverse linear correlation between  $V_{O_2}$  and buffer NO concentration was present in control tissue (Fig. 3). A similar, but significantly stronger ( $p < 0.05$  by Fischer z-test) correlation was present in the NEC-healthy tissue (Fig. 4). The buffer concentrations of NO were higher in the NEC-healthy group and a bimodal distribution of NO data was evident. This circumstance is consistent with the induction of iNOS in this tissue, which generates NO at a rate substantially greater than the other NOS isoforms. A correlation between  $V_{O_2}$  and buffer NO concentration was not present in the NEC-diseased tissue (Fig. 5). No correlation was noted between  $V_{O_2}$  in NEC-healthy or NEC-diseased tissues and the duration of feeding, maximal feeding volume achieved, and hours of enteral fasting before laparotomy (data not shown). A direct linear correlation was noted between gestational age and baseline  $V_{O_2}$  in control tissue (Fig. 6), but not from NEC tissues (data not shown).

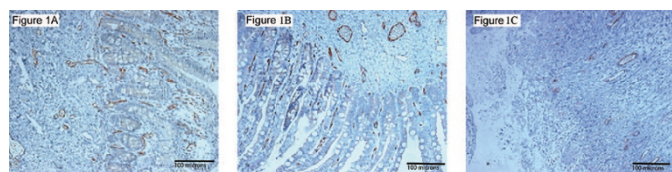


**Figure 1.** Immunostaining for eNOS. All photomicrographs shown at 200 $\times$ . The photomicrographs shown are representative of all control, NEC-healthy, and NEC-diseased tissue specimens. (A) Control tissue: Staining is evident in the endothelial lining of the submucosal arterioles and venules, as well as in the villus microvessels. (B) NEC-healthy tissue: Staining is very similar to that noted in the control tissue, *i.e.* present in the endothelial lining of the submucosal and villus microvessels. (C) NEC-diseased tissue: Staining is present to a modest degree in the submucosal microvessels, but the submucosal microcirculation has been destroyed.

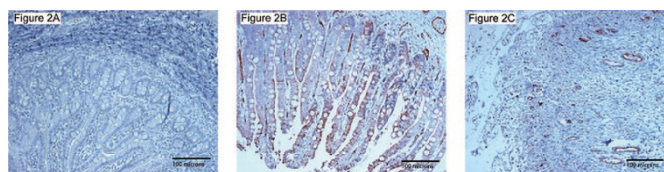


**Figure 2.** Immunostaining for iNOS. All photomicrographs shown at 200 $\times$ . The photomicrographs shown are representative of all control, NEC-healthy, and NEC-diseased tissue specimens. (A) Control tissue: No staining for iNOS is evident. (B) NEC-healthy tissue: Abundant staining is evident, particularly within villus enterocytes. Staining is also present in the microvascular elements of the submucosa and villi. This staining was not nonspecific, *i.e.* it was not present when only the 2<sup>o</sup> antibody was applied. (C) NEC-diseased tissue: A modest amount of staining is present, particularly noted in the microvasculature within the submucosa.

**Table 2.** Intestinal  $V_{O_2}$  in human tissue

	NEC		
	Control	Healthy	Diseased
Baseline	396 $\pm$ 26	200 $\pm$ 22 $\dagger$	184 $\pm$ 19 $\dagger$
L-NIL ( $10^{-4}$ M)	389 $\pm$ 39	380 $\pm$ 25*	215 $\pm$ 27 $\ddagger$
L-NNA ( $5 \times 10^{-8}$ M)	393 $\pm$ 29	216 $\pm$ 19 $\dagger$	216 $\pm$ 25 $\dagger$
SP ( $10^{-8}$ M)	364 $\pm$ 42	218 $\pm$ 21 $\dagger$	235 $\pm$ 64 $\dagger$
SNAP ( $^{-4}$ M)	200 $\pm$ 32*	158 $\pm$ 28* $\dagger$	164 $\pm$ 20 $\dagger$

Data are expressed as nM  $O_2$ /min/g and mean  $\pm$  SD,  $n = 7$  for control group,  $n = 14$  for NEC group. Analysis by two-way ANOVA, significance set at  $p < 0.01$ : \* drug *vs* baseline;  $\dagger$  NEC *vs* control;  $\ddagger$  NEC-diseased *vs* NEC-healthy.

**Table 3.** Intestinal NO production in human tissue

	NEC		
	Control	Healthy	Diseased
Baseline	46 $\pm$ 16	138 $\pm$ 25 $\dagger$	48 $\pm$ 7 $\ddagger$
L-NIL ( $10^{-4}$ M)	43 $\pm$ 14	33 $\pm$ 10*	39 $\pm$ 7
L-NNA ( $5 \times 10^{-8}$ M)	39 $\pm$ 13	136 $\pm$ 21 $\dagger$	43 $\pm$ 5 $\ddagger$
SP ( $10^{-8}$ M)	66 $\pm$ 14	98 $\pm$ 14 $\dagger$	53 $\pm$ 7 $\ddagger$
SNAP ( $10^{-4}$ M)	126 $\pm$ 8*	187 $\pm$ 16* $\dagger$	146 $\pm$ 12*

Data are expressed as nM NO/ $\mu$ L/g and mean  $\pm$  SD,  $n = 7$  for control group,  $n = 14$  for NEC group. Analysis by two-way ANOVA, significance set at  $p < 0.01$ : \* drug *vs* baseline;  $\dagger$  NEC *vs* control;  $\ddagger$  NEC-diseased *vs* NEC-healthy.

## DISCUSSION

The study hypothesis, that iNOS-derived NO suppresses  $V_{O_2}$  in human intestine resected for NEC was predicated on the established capacity of NO to compromise mitochondrial respiration. NO reversibly inhibits cytochrome *c*, the terminal step in the electron transport chain (9). This effect occurs within physiologically relevant NO concentrations; thus, the  $K_i$  for NO inhibition of mitochondrial respiration is approximately 27 nM (22), a level similar to that noted in the periarteriolar interstitium (23). Endogenously derived NO depresses myocardial  $V_{O_2}$  and this response appears to participate in the normal physiologic regulation of cardiac function (24). In healthy myocardial tissue, the source of the NO that modulates tissue  $V_{O_2}$  is eNOS that is present within arteriolar endothelial cells immediately adjacent to myocytes (10). eNOS-derived NO did not affect intestinal  $V_{O_2}$ , as evidenced

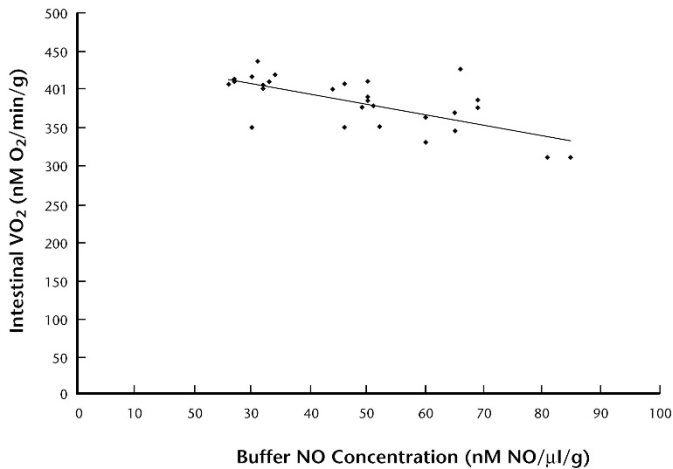


**Figure 3.** Correlation between buffer NO concentration and intestinal  $V_{O_2}$  for control tissue.  $y = 1.37x + 448$ ;  $n = 28$ ,  $R^2 = 0.45$ ,  $p < 0.05$ .

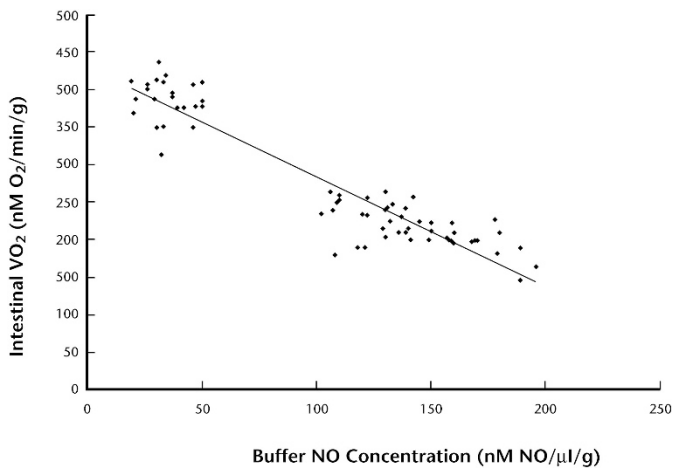


**Figure 4.** Correlation between buffer NO concentration and intestinal  $V_{O_2}$  for NEC-healthy tissue.  $y = -1.45x + 428$ ;  $n = 56$ ,  $R^2 = 0.88$ ,  $p < 0.001$ . Note that the scale for the  $x$  axis is expanded with respect to Figures 3 and 5, reflecting the greater accumulation of NO into the buffer bathing medium under baseline conditions. The significance of the correlation coefficient was greater in NEC-healthy tissue than in control tissue (Fischer  $z$ -test).

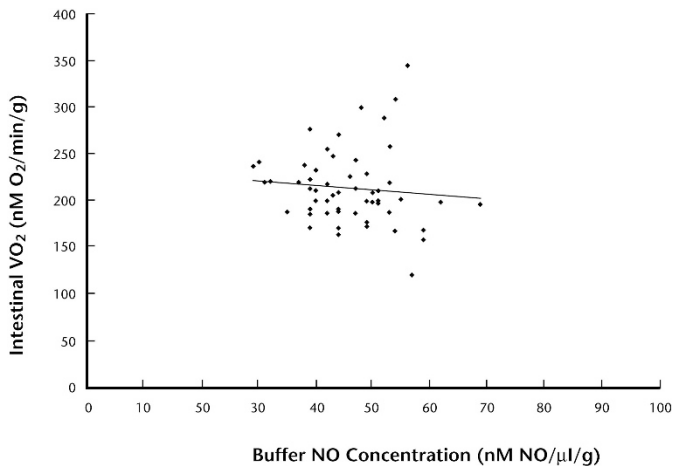


**Figure 5.** Correlation between buffer NO concentration and intestinal  $V_{O_2}$  for NEC-diseased tissue.  $y = -0.48x + 237$ ;  $n = 28$ ,  $R^2 = 0.009$ , NS.

by the failure of SP or L-NNA to alter  $V_{O_2}$ . However, the SNAP data demonstrate that NO-induced depression of intestinal  $V_{O_2}$  can occur.

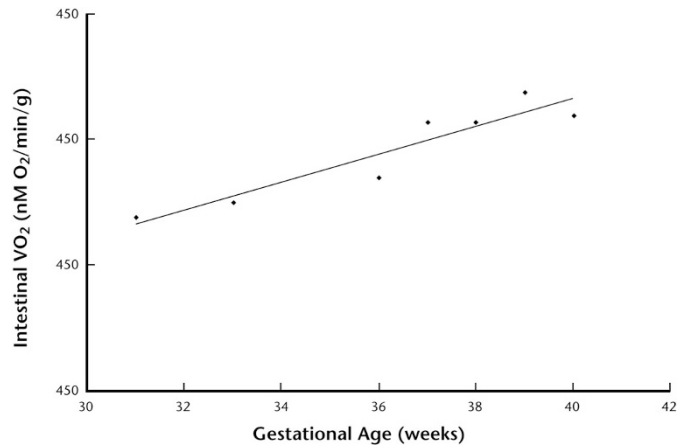


**Figure 6.** Correlation between gestational age and baseline  $V_{O_2}$  for control tissue.  $y = 5.61x + 192$ ;  $n = 7$ ,  $R^2 = 0.88$ ,  $p < 0.01$ .

Suppression of intestinal  $V_{O_2}$  by iNOS-derived NO was clearly evident in NEC-healthy tissue. The baseline  $V_{O_2}$  was depressed in NEC-healthy tissue, whereas the concentration of NO in conditioned buffer was significantly greater in this tissue group; moreover, a strong correlation between buffer NO concentration and intestinal  $V_{O_2}$  was evident. That the source of this NO was iNOS was supported by two observations: first, a marked up-regulation of iNOS expression was evident in all NEC-healthy specimens and, second, L-NIL, reduced accumulation of NO into the buffer and simultaneously increased  $V_{O_2}$ .

The aforementioned observations may be relevant to the pathogenesis of NEC. Up-regulation of iNOS was most conspicuous in the villi. The villi are the principal site of  $O_2$  utilization in the intestine, a circumstance that renders them most susceptible to functional disruption or damage in the presence of dysoxia, whether generated by compromise in  $O_2$  availability or by the capacity of the mitochondria to use  $O_2$  in oxidative phosphorylation (25). The villi are also the location of the earliest histopathological lesions of NEC (26). Beltran *et al.* (27) demonstrated that NO-induced depression of mitochondrial respiration was sufficient to induce enterocyte apoptosis, and Ford and colleagues (1) showed apoptosis to be present in human intestine resected for NEC. Combining these observations, we speculate that depression of intestinal  $V_{O_2}$  via iNOS-derived NO may contribute to enterocyte damage, necrosis, or apoptosis and that this process occurs very early in the pathogenesis of NEC. This speculation is consistent with demonstration of iNOS up-regulation and reversible NO-induced depression of intestinal  $V_{O_2}$  in areas of the intestine that demonstrate relatively intact architecture, *i.e.* in areas of the intestine immediately adjacent to regions of overt necrosis.

Interestingly, no evidence of an interaction between NO and  $V_{O_2}$  was observed in NEC-diseased tissue, *i.e.* tissue that demonstrated significant histopathological evidence of NEC, nor was the low  $V_{O_2}$  of this tissue reversed by L-NIL. The tissue injury score here was substantial: villus sloughing, coagulation necrosis, and vascular congestion of the microcirculation (which itself implies downstream ischemia) were consistently present in all specimens. We thus speculate that

the low  $V_{O_2}$  in this tissue reflected a loss of viable (*i.e.*  $O_2$  consuming) tissue. Inclusion of these observations in this report serves to confirm that the interaction between iNOS-derived NO and  $V_{O_2}$  was localized to tissue that appeared viable NEC-healthy tissue, and that the interaction might thus reflect a relevant pathogenetic mechanism rather than an artifact representative of dead or dying tissue.

Two caveats to these data deserve discussion. First, the control and NEC patient groups were not alike; most significantly, the gestational age of the NEC patients was significantly lower than that of the control patients. This difference could present a problem insofar as a direct linear correlation between baseline  $V_{O_2}$  and gestational age was evident in the control group (Fig. 6), suggesting that gut  $V_{O_2}$  is lower in preterm infants in the absence of disease. Is it possible, therefore, that the lower baseline  $V_{O_2}$  noted in NEC patients was the consequence of normal developmental physiology (*i.e.* secondary to prematurity) rather than a pathophysiological process (*i.e.* secondary to NEC)? We reject this possibility insofar as  $V_{O_2}$  in NEC-healthy infants significantly increased (to nearly the level of control infants) after L-NIL administration, suggesting that the depression was secondary to a reversible, NO-based effect, rather than a developmental phenomenon. The second caveat is that none of the control infants had been fed, while all of the NEC patients had received enteral nutrition for several days before the onset of disease. Feeding affects gut  $V_{O_2}$ ; specifically, the active transport processes initiated by luminal nutrients significantly increase  $V_{O_2}$  (25). Luminal nutrients also serve as a stimulant for growth in the perinatal intestine (28). In this context, however, baseline  $V_{O_2}$  was significantly lower in NEC (fed) than control (not fed) infants, a pattern opposite of that predicted based solely on the effects of luminal nutrients on gut  $V_{O_2}$ .

It is important to recognize that NO has also been proposed to prevent the development of NEC, possibly because of the vasodilator effect of NO in the newborn intestinal circulation. Indeed, we have previously proposed loss of intestinal vascular eNOS activity as the basis for the microvascular ischemia that appears to occur in NEC (29). Blockade of eNOS activity aggravates intestinal injury generated by platelet activating factor, a proinflammatory lipid mediator present in infants with NEC (30,31). Clinical studies demonstrate that L-arginine, the substrate used by all NOS in the generation of NO is low in the plasma of infants with NEC when compared with age-matched controls (32,33), and Amin *et al.* (34) reported that L-arginine supplementation reduced the incidence of NEC in infants  $\leq 1250$  g. It is feasible, however, that the beneficial effect of L-arginine was unrelated to an enhancement eNOS-derived NO, insofar as L-arginine is also the precursor for glutamine and glutamate that serve as metabolic fuels for enterocytes (35). As well, L-arginine stimulates enterocyte migration *via* NO and focal adhesion kinase pathways and thus may be important in wound repair in NEC (36).

In summary, we have demonstrated that tissue  $V_{O_2}$  is depressed, whereas tissue release of NO into bathing buffer is increased in gut resected from preterm infants for NEC that has a relatively normal histologic appearance. Immunohistochemistry and selective pharmacological blockade impli-

cate iNOS as the source of this NO. We propose that suppression of tissue  $V_{O_2}$  is yet one more means whereby iNOS-derived NO contributes to the pathogenesis of NEC.

## REFERENCES

1. Ford H, Watkins S, Reblock K, Rowe M 1997 The role of inflammatory cytokines and nitric oxide in the pathogenesis of necrotizing enterocolitis. *J Pediatr Surg* 32:275–282
2. Nadler EP, Dickinson E, Knisley A, Zhang XR, Boyle P, Beer-Stolz D, Watkins SC, Ford HR 2000 Expression of inducible nitric oxide synthase and interleukin-12 in experimental necrotizing enterocolitis. *J Surg Res* 92:71–77
3. Hierholzer C, Kalf JC, Billiar TR, Bauer AJ, Tweardy DJ, Harbrecht BG 2004 Induced nitric oxide promotes intestinal inflammation following hemorrhagic shock. *Am J Physiol Gastrointest Liver Physiol* 286:G225–G233
4. Dickinson E, Tuncer R, Nadler E, Boyle P, Alber S, Watkins S, Ford H 1999 NOX, a novel nitric oxide scavenger, reduces bacterial translocation in rats after endotoxin challenge. *Am J Physiol* 277:G1281–G1287
5. Suzuki Y, Deitch EA, Mishima S, Lu Q, Xu D 2000 Inducible nitric oxide synthase gene knockout mice have increased resistance to gut injury and bacterial translocation after an intestinal ischemia-reperfusion injury. *Crit Care Med* 28:3692–3696
6. Deitch EA, Shorshtein A, Houghton J, Lu Q, Xu D 2002 Inducible nitric oxide synthase knockout mice are resistant to diet-induced loss of gut barrier function and intestinal injury. *J Gastrointest Surg* 6:599–605
7. Rachmilewitz D, Stamler JS, Bachwich D, Karmeli F, Ackerman Z, Podolsky DK 1995 Enhanced colonic nitric oxide generation and nitric oxide synthase activity in ulcerative colitis and Crohn's disease. *Gut* 36:718–723
8. Kankuri E, Hamalainen M, Hukkanen M, Salmenpera P, Kivilaakso E, Vapaatalo H, Moilanen E 2003 Suppression of pro-inflammatory cytokine release by selective inhibition of inducible nitric oxide synthase in mucosal explants from patients with ulcerative colitis. *Scand J Gastroenterol* 38:186–192
9. Cleeter MW, Cooper JM, Darley-Usmar VM, Moncada S, Schapira AH 1994 Reversible inhibition of cytochrome c oxidase, the terminal enzyme of the mitochondrial respiratory chain, by nitric oxide. Implications for neurodegenerative diseases. *FEBS Lett* 345:50–54
10. Loke KE, McConnell PI, Tuzman JM, Shesely EG, Smith CJ, Stackpole CJ, Thompson CI, Kaley G, Wolin MS, Hintze TH 1999 Endogenous endothelial nitric oxide synthase-derived nitric oxide is a physiological regulator of myocardial oxygen consumption. *Circ Res* 84:840–845
11. Laycock SK, Vogel T, Forfia PR, Tuzman J, Xu X, Ochoa M, Thompson CI, Nasjletti A, Hintze TH 1998 Role of nitric oxide in the control of renal oxygen consumption and the regulation of chemical work in the kidney. *Circ Res* 82:1263–1271
12. Wolin MS, Hintze TH, Shen W, Mohazzab-HKM, Xie YW 1997 Involvement of reactive oxygen and nitrogen species in signalling mechanisms that control tissue respiration in muscle. *Biochem Soc Trans* 25:934–939
13. Nowicki PT 1998 Postnatal changes in gut hemodynamics: a possible role for substance P. *Am J Physiol* 274:G1142–G1150
14. Potoka DA, Nadler EP, Zhou X, Zhang XR, Upperman JS, Ford HR 2000 Inhibition of NF-kappaB by IkappaB prevents cytokine-induced NO production and promotes enterocyte apoptosis *in vitro*. *Shock* 14:366–373
15. Furfine ES, Harmon MF, Paith JE, Garvey EP 1993 Selective inhibition of constitutive nitric oxide synthase by L-NG-nitroarginine. *Biochemistry* 32:8512–8517
16. Zhang JY, Wang Y, Milton MN, Kraus L, Breau AP, Paulson SK 2004 Disposition and pharmacokinetics of L-N6-(1-iminoethyl)lysine-5-tetrazole-amide, a selective iNOS inhibitor, in rats. *J Pharm Sci* 93:1229–1240
17. Xie YW, Shen W, Zhao G, Xu X, Wolin MS, Hintze TH 1996 Role of endothelium-derived nitric oxide in the modulation of canine myocardial mitochondrial respiration *in vitro*. Implications for the development of heart failure. *Circ Res* 79:381–387
18. Nowicki PT, Miller CE 1993 Regulation of capillary exchange capacity in postnatal swine intestine. *Am J Physiol* 265:G1090–G1097
19. Reber KM, Mager GM, Miller CE, Nowicki PT 2001 Relationship between flow rate and NO production in postnatal mesenteric arteries. *Am J Physiol Gastrointest Liver Physiol* 280:G43–G50
20. Book LS, Overall Jr, JC Herbst, JJ, Britt MR, Epstein B, Jung AL 1977 Clustering of necrotizing enterocolitis. Interruption by infection-control measures. *N Engl J Med* 297:984–986
21. Sommerschildt HC 1971 Intestinal perforation in the newborn infant as a complication in umbilical vein infusion or exchange transfusion. *Surgery* 70:609–613
22. Koivisto A, Mathias A, Bronnikov G, Nedergaard J 1997 Kinetics of the inhibition of mitochondrial respiration by NO. *FEBS Lett* 417:75–80
23. Bohlen HG 1998 Mechanism of increased vessel wall nitric oxide concentrations during intestinal absorption. *Am J Physiol* 275:H542–H550
24. Shen W, Hintze TH, Wolin MS 1995 Nitric oxide. An important signaling mechanism between vascular endothelium and parenchymal cells in the regulation of oxygen consumption. *Circulation* 92:3505–3512
25. Bohlen HG 1980 Intestinal mucosal oxygenation influences absorptive hyperemia. *Am J Physiol* 239:H489–H493
26. Ballance WA, Dahms BB, Shenker N, Kliegman RM 1990 Pathology of neonatal necrotizing enterocolitis: a ten year experience. *J Pediatr* 117:S6–S13

27. Beltrán B, Mathur A, Duchon MR, Erusalimsky JD, Moncada S 2000 The effect of nitric oxide on cell respiration: a key to understanding its role in cell survival or death. *Proc Natl Acad Sci U S A* 97:14602–14607
28. Widdowson EM 1985 Development of the digestive system: comparative animal studies. *Am J Clin Nutr* 41:384–390
29. Reber KM, Nankervis CA, Nowicki PT 2002 Newborn intestinal circulation. *Physiology and pathophysiology. Clin Perinatol* 29:23–39
30. MacKendrick W, Caplan M, Hsueh W 1993 Endogenous nitric oxide protects against platelet-activating factor-induced bowel injury in the rat. *Pediatr Res* 34:222–228
31. Caplan MS, Sun XM, Hsueh W, Hageman JR 1990 Role of platelet activating factor and tumor necrosis factor-alpha in neonatal necrotizing enterocolitis. *J Pediatr* 116:960–964
32. Becker RM, Wu G, Galanko JA, Chen W, Maynor AR, Bose CL, Rhoads JM 2000 Reduced serum amino acid concentrations in infants with necrotizing enterocolitis. *J Pediatr* 137:785–793
33. Zamora SA, Amin HJ, McMillan DD, Kubes P, Fick GH, Butzner JD, Parsons HG, Scott RB 1997 Plasma L-arginine concentrations in premature infants with necrotizing enterocolitis. *J Pediatr* 131:226–232
34. Amin HJ, Zamora SA, McMillan DD, Fick GH, Butzner JD, Parsons HG, Scott RB 2002 Arginine supplementation prevents necrotizing enterocolitis in the premature infant. *J Pediatr* 140:425–431
35. Neu J 2002 Arginine supplementation and the prevention of necrotizing enterocolitis in very low birth weight infants. *J Pediatr* 140:389–391
36. Rhoads JM, Chen W, Gookin J, Wu GY, Fu Q, Blikslager AT, Rippe RA, Argenzio RA, Cance WG, Weaver EM, Romer LH 2004 Arginine stimulates intestinal cell migration through a focal adhesion kinase dependent mechanism. *Gut* 53:514–522